Blockade of the Ras/Raf/ERK and Ras/PI3K/Akt pathways by monacolin K reduces the expression of GLO1 and induces apoptosis in U937 cells

ARTICLE *in* JOURNAL OF AGRICULTURAL AND FOOD CHEMISTRY · JANUARY 2015

Impact Factor: 2.91 · DOI: 10.1021/jf505275s · Source: PubMed

JOURNAL OF AGRICULTURAL AND FOOD CHEMISTRY

Article

pubs.acs.org/JAFC

Blockade of the Ras/Raf/ERK and Ras/PI3K/Akt Pathways by Monacolin K Reduces the Expression of GLO1 and Induces Apoptosis in U937 Cells

Chun-Chia Chen,[†] Mei-Li Wu,[†] Chi-Tang Ho,[§] and Tzou-Chi Huang*[,†]

[†]Department of Food Science, National Pingtung University of Science and Technology, Pingtung 91201, Taiwan

[§]Department of Food Science, Rutgers University, New Brunswick, New Jersey 08901, United States

ABSTRACT: Monacolin K, a hydrolytic product of icaritin, is the major active component in the traditional fermented *Monascus purpureus*. Monacolin K inhibits the proliferation of acute myeloid leukemia (AML), but underlying mechanisms remain to be identified. The present study demonstrates that monacolin K inhibits the proliferation of human AML cell line U937 in a dose-dependent manner. Importantly, morphological, DNA fragmentation, and image cytometry analyses indicated that monacolin K induced U937 cell apoptosis. Monacolin K could inactivate Ras translocation from cytosol to cell membrane. Monacolin K could also reduce the Ras-dependent phosphorylation of ERK and Akt, and the subsequent translocation of nuclear factor kappa B (NF-κB) from cytosol to nucleus in U937 cells. The underlying mechanisms of apoptotic activity of monacolin K were associated with inhibition of the Ras/Raf/ERK and Ras/PI3K/Akt signals and down-regulation of HMG-CoA reductase and glyoxalase 1. On the basis of results obtained using specific inhibitors U0126, LY294002, and JSH-23, the Ras/Raf/ERK/NF-κB/GLO1 and Ras/Akt/NF-κB/GLO1 pathways were proposed for the apoptotic effect of monacolin K in U937 cells.

KEYWORDS: *monacolin K, acute myeloid leukemia, glyoxalase 1, HMG-CoA reductase, inactivate Ras translocation, apoptosis*

INTRODUCTION

Red yeast rice (RYR) is a traditional fermented product of *Monascus purpureus* and white rice.[1] It is popular in some Asian countries and is known to have properties of lowering total cholesterol (TC) and low-density lipoprotein-cholesterol (LDL-C) levels.[2] Accumulating evidence has also shown that RYR inhibited proliferation of various cancer cells in vitro.[3,4] The major bioactive compound in RYR, monacolin K, also showed tumor-suppressive activity in animal models.[5] RYR is a potentially useful over-the-counter cholesterol-lowering agent. The typical RYR dose used in clinical trials is 1200−2400 mg/day, which contains approximately 5 mg of monacolin K.[2]

The structure of monacolin K is identical to that of the statin drug lovastatin. Case reports and early clinical studies suggest a therapeutic potential for statins in acute myeloid leukemia (AML). Statins are 3-hydroxy-3-methylglutaryl-coenzyme A reductase (HMGCR) inhibitors that act on the mevalonate pathway and inhibit synthesis of cholesterol, geranylgeranyl pyrophosphate (GGPP), and farnesyl pyrophosphate (FPP).[6] It is well established that mevalonate is essential for post-translational modification of Ras, which can lead to increased levels of farnesylation of Ras by farnesyl-pyrophosphate transferase. Inhibition of mevalonate synthesis leads to a depletion of its downstream intermediates, such as FPP and GGPP, precursors for sterols, dolichols, coenzyme Q, isoprenoids, and carotenoids.[7] FPP and GGPP are substrates for the post-translational modification of proteins including the Ras and Rho family GTPases, well-known proto-oncogenes for the control of cell growth, migration, survival, and differentiation in mammalian cells. Statins inactivate Ras translocation and downstream MEK/ERK and PI3K/Akt signalings leading to cancer cell apoptosis by interrupting the biosynthesis of mevalonate.[8] Genetic mutations of Ras protein in cancer cells trigger dysregulation of Ras/Raf/MEK/ERK and Ras/PI3K/PTEN/Akt/mTOR pathway signalings, leading to uncontrolled cellular proliferation and decreased sensitivity to agents that ordinarily can trigger apoptosis.

It is well established that glyoxalase 1 (GLO1) plays a pivotal role in the growth and survival of cancer cells. GLO1 is a key enzyme for protecting cancer cells from apoptosis, and it works through the elimination of excess methylglyoxal (MG), which is a toxic metabolite of the major energy source, glucose. The increased survival activity of tumors, including higher glycolytic activity and a consequent rise in MG production, requires an increased detoxifying action of GLO1.[9] The increase of GLO1 expression has been shown to be associated with increased proliferative activity of tumors. In antitumor agent-resistant leukemia cells, GLO1 was frequently overexpressed.[10] Immunohistochemical analysis confirmed the increase of GLO1 among patients with colon carcinoma[11] or prostate cancer.[12] Significantly high glyoxalase activity has been detected during differentiation of leukemia cells.[13] Endogenously produced MG has been shown to cause apoptosis in cultured leukemia cells.[14]

In contrast with that in normal cells, the cholesterol content of malignant tumors in the body is particularly high. The primary source of cholesterol synthesis in cancer cells is glucose. Cholesterol is currently known to be synthesized from a series of reactions involving the conversion of citrate in the tricarboxylic acid (TCA) cycle to generate acetyl coenzyme A,

Received: November 1, 2014
Revised: January 5, 2015
Accepted: January 8, 2015
Published: January 8, 2015

DOI: 10.1021/jf505275s
J. Agric. Food Chem. 2015, 63, 1186−1195

which then reacts with several enzymes in the mevalonate pathway to yield cholesterol.[15] It is well established that HMGCR activity was 3-fold higher in mononuclear blood cells from patients with leukemia, compared with cells from healthy subjects.[16]

We here provide a detailed mechanistic investigation of the apoptotic effect of monacolin K and how it is related to the inhibition of GLO1. In the present study, we hypothesize that monacolin K showed its apoptotic activity through the inhibition of HMGCR, inactivation of Ras translocation, and down-regulation of PI3K/Akt and Raf/ERK1/2 signal pathways, leading to suppression of GLO1 and HMGCR in U937 cells.

MATERIALS AND METHODS

Chemicals and Antibodies. Monacolin K, perchloric acid, 2-methylquinoxaline (2-MQ), *o*-phenylenediamine, 3-(4,5-dimethylthiazol-2-y-l)-2,5-diphenyltetrazolium bromide (MTT), dimethyl sulfoxide (DMSO), and 4,6-diamidino-2-phenylindole (DAPI) were purchased from Sigma-Aldrich (St. Louis, MO, USA). Cell culture media were purchased from Invitrogen (Carlsbad, CA, USA). Antibodies against phospho-p44/42 MAPK (Thr202/Tyr204), phospho-Akt (Ser473), ERK1/2, Akt1/PKBα, and actin, were obtained from Millipore (Billerica, MA, USA). Antibodies against GLO-1, NF-κB (p65), H-Ras, Raf-1, and lamin A were obtained from Santa Cruz Biotechnology (Santa Cruz, CA, USA). Antibodies against K-Ras and N-Ras were obtained from GeneTex (San Antonio, TX, USA). Alexa Fluor 594 goat anti-mouse IgG (H+L) was purchased from Invitrogen. U0126 (MEK1/2 inhibitor), LY294002 (PI3K inhibitor), JSH-23 (NF-κB inhibitor), IgG HRP-conjugated goat anti-mouse and IgG HRP-conjugated goat anti-rabbit were obtained from Chemicon (Temecula, CA, USA).

Cell Culture. U937 cells were purchased from the American Type Culture Collection (Rockville, MD, USA). The cells were cultured in RPMI 1640 medium with 10% fetal bovine serum (GibcoBRL, Grand Island, NY, USA), 5 mM L-glutamine (GibcoBRL), and 1% penicillin/streptomycin (10000 units of penicillin/mL and 10 mg/mL streptomycin) at 37 °C in a humidified 5% CO_2 incubator.

Cell Viability Assay. Cell viability was assessed by MTT assay.[17] Briefly, cells at 1×10^5/mL were treated with various concentrations of monacolin K in 96-well plates for 48 h, followed by treatment with MTT for 4 h at 37 °C. The medium was removed, DMSO was added to dissolve the blue formazan residue, and color intensity was measured using an ELISA reader at 570 nm.

Morphological Assay. After treatment with various concentrations of monacolin K for 48 h, cells were harvested and fixed with 4% paraformaldehyde in PBS for 20 min at room temperature and stained with 2.5 mg/mL DAPI solution for 30 min at room temperature. The cells were washed two more times with PBS and analyzed via a confocal microscope (CARV II Confocal Imager; BD Biosciences).

DNA Fragmentation Assay. After treatment with various concentrations of monacolin K for 48 h and washing with ice-cold PBS, the cells were resuspended in 180 μL of DNA lysis buffer (0.5% lauroylsarcosine, 10 mM EDTA, 0.5 mg/mL proteinase K, and 50 mM Tris-HCl at pH 8.0) overnight at 56 °C and treated with RNaseA (0.5 μg/mL) for 1 h at 37 °C. Total DNA was extracted from the cells with an equal volume of phenol/chloroform/isoamyl alcohol (Sigma-Aldrich). Ten microliters of DNA was analyzed on 1.8% agarose gel.

Image Cytometry Analysis. Cell sub-G1 phase was analyzed by the DNA content using the DAPI staining method. After treatment with various concentrations of monacolin K for 48 h, U937 cells were centrifuged at 1500 rpm for 5 min, and the cell pellets were fixed in 70% ice-cold ethanol overnight at 4 °C. Fixed cells were washed with PBS, incubated with 0.5 mL of hypotonic buffer containing 0.5% Triton X-100 and 0.5 mg/mL RNase A for 30 min at 37 °C, and then stained with 50 μg/mL DAPI, and the sub-G1 phase content was determined on a NucleoCounter NC-3000 cytometer (ChemoMetec, Allerod, Denmark).

RNA Isolation and Reverse Transcription-PCR Amplification (RT-PCR). Total RNA was extracted from U937 cells using a commercially available RNA extraction kit (Favorgen, Pingtung, Taiwan) and following the manufacturer's instruction. First-stranded cDNA was synthesized using 1 μg of total RNA by RT-PCR kit (Roche, Indianapolis). The relative expressions of GLO1 and HMGCR were analyzed using RT-PCR with GAPDH as an internal control. The primers used were GLO1, sense 5′-ATGGCAGAACCGCAGCCCCCGT-3′ and antisense 5′-CTACATTAAGGTTGCCATTTTGTTAG-3′, yielding a product of length 564 bp; HMGCR, sense 5′-TACCATGTCAGGGGTACGTC-3′ and antisense 5′-CAAGCCTAGAGACATAATCATC-3′, yielding a product of length 252 bp; GAPDH, sense 5′-TACCATGTCAGGGGTACGTC-3′ and antisense 5′-CAAGCCTAGAGACATAATCATC-3′, yielding a product of length 248 bp. A 10 μL volume reaction for PCR included 2 μL of cDNA, 1 μL each of sense and antisense primers, and 5 μL of PCR master mix. The conditions were 94 °C for 5 min, 94 °C for 40 s, 60 °C for 35 s (GLO1), 58 °C for 30 s (HMGCR), and 64 °C for 30 s (GAPDH), 72 °C for 40 s, and 72 °C for 7 min, for 26 cycles. The PCR products were separated by electrophoresis on 1.5% agarose gels, and the results were analyzed using a Kodak Gel logic imaging system (Hyland Scientific, Stanwood, WA, USA).

Western Blot Analysis. The whole cell protein was extracted via the addition of 100 μL of gold lysis buffer (50 mM Tris-HCl, 150 mM NaCl, 1 mM EDTA, 1% Triton X-100, and 1% protease inhibitor cocktail at pH 7.4), followed by incubation at 4 °C for 1 h, centrifugation, and collection of cell lysate. A Subcellular Protein Fractionation Kit was used to determine the levels of protein expression in cytosol, nucleus, and membrane. Extract preparation followed instruction of the manufacturer's published protocol (Thermo, Rockford, IL, USA). Protein concentrations were measured with a Bio-Rad protein assay reagent (Bio-Rad Laboratories, Munich, Germany). Equal amounts of lysate protein (30 μg/lane) were subjected to sodium dodecyl sulfate–polyacrylamide gel electrophoresis (SDS-PAGE). After electrophoresis, the proteins were electrotransferred to polyvinylidene difluoride (PVDF) membranes (Millipore, Billerica, MA, USA), blocked at 37 °C for 1 h with 1% BSA in TBST (20 mM/L Tris-base; 125 mM/L NaCl; 0.2% Tween 20; 0.1% sodium azide), then immunoblotted with primary antibodies overnight at 4 °C, and washed with TBST solution (0.05% Tween 20 in TBS). After six washings with TBST buffer, the blot was washed and exposed to horseradish peroxidase conjugated secondary antibodies for 1 h, and immunoreactive proteins were visualized with an enhanced chemiluminescence (ECL) detection system (GE Healthcare, Little Chalfont, UK).

Total Cholesterol Quantitation. The total cholesterol concentration was measured using a Cholesterol/Cholesterol Ester Quantitation Kit (Calbiochem, Novabiochem, Boston, MA, USA). After treatment with monacolin K for 48 h, cells were washed with cold PBS and centrifuged. The pellet was resuspended in 0.2 mL of chloroform/isopropanol/NP-40, homogenized for 3 min, and cleared by centrifugation at 14000 rpm for 10 min. Supernatants were decanted, air-dried at 50 °C, and vacuum-dried for 30 min to remove residual solvents. The dried lipids were dissolved in 0.2 mL of the reaction buffer, and the absorbance was measured at 570 nm for total cholesterol detection.

Methylglyoxal Measurement. MG was measured by using an *o*-phenylenediamine method.[18] MG was derivatized with *o*-phenylenediamine to form the quinoxaline product 2-MQ, which is very specific for MG. Briefly, the supernatant of the cell was incubated with 100 mM *o*-phenylenediamine for 3 h at room temperature. The quantity of the quinoxaline derivative of MG (2-MQ) was measured using a Hitachi L-6200 HPLC system (Hitachi, Ltd., Mississauga, ON, Canada). The mobile phase was generally 68 vol % of 10 mM KH_2PO_4 (pH 2.5) and 32 vol % of HPLC grade acetonitrile. The analysis conditions were as follows: detector wavelength, 315 nm; mobile phase flow rate, 1.0 mL/min; and column temperature, 20 °C. The whole series of samples in a single experiment was run in duplicate.

Immunofluorescence Microscopy. To detect the localization of NF-κB in monacolin K treated U937 cells, the U937 cells were first seeded in a 12-well dish. The cells were fixed with 4% paraformaldehyde

DOI: 10.1021/jf505275s
J. Agric. Food Chem. 2015, 63, 1186−1195

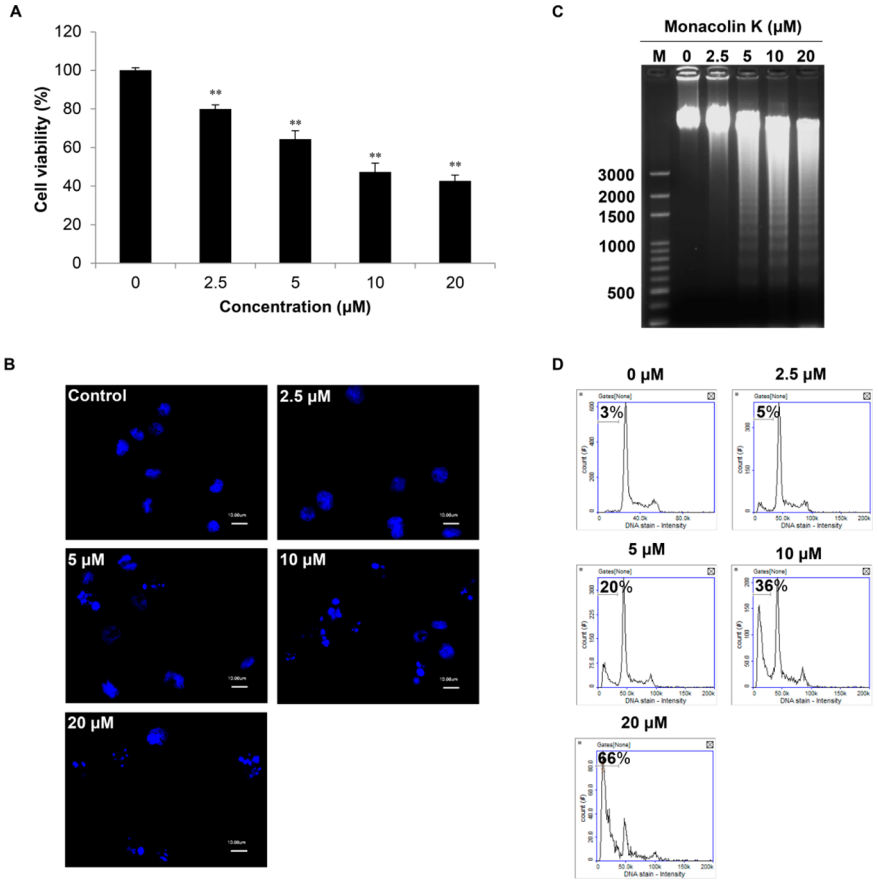

Figure 1. Inhibition of cell viability and apoptosis-inducing effects of monacolin K on U937 cells. (A) U937 cells were seeded (1×10^5 cells/well) in a 96-well plate, the cells were treated with variable concentrations of monacolin K for 48 h, and cell viability was measured by MTT assay. (B) Nuclear condensation in apoptotic cells detected by DAPI staining. U937 cells were treated with various concentrations of monaclin K for 48 h. (C) DNA fragmentation was detected by gel electrophoresis following stimulation with 2.5−20 μM monacolin K for 48 h. (D) Image cytometry analysis shows the percentage of sub-G1 phase in U937 cells treated with monacolin K for 48 h. All data represent means ± SD of triplicates (n = 3). In panel A, ** $p < 0.01$, compared with untreated cells (control groups).

for 30 min and permeabilized with PBS containing 0.1% Triton X-100 for 5 min at room temperature. After specimens were blocked with 5% BSA for 1 h at room temperature, they were further incubated with NF-κB (p65) antibody for 2 h. After three washings in TPBS, specimens were then stained with Alexa Fluor 594 goat anti-mouse IgG for 1 h at room temperature. After three washings with TPBS, cells were stained with 0.5 mg/mL of DAPI for 10 min to counterstain the nucleus and then washed three times for 5 min with TPBS. Images were collected by confocal microscope.

Statistical Analysis. The data were analyzed using the SAS program (SAS Institute, Cary, NC, USA). The significance of the difference among mean values was determined by one-way analysis of variance followed by the t test; (*) $p < 0.05$ and (**) $p < 0.01$ were considered statistically significant. Values are the mean ± SD of three independent experiments.

RESULTS

Monacolin K Induced Apoptosis in U937 Cells. MTT assays were performed to evaluate the potential cytotoxic effects of monacolin K. As shown in Figure 1A, U937 cells were incubated with increased concentrations of monacolin K for 48 h. Exposure of monacolin K to U937 cells resulted in a significant decrease in viable cells in a dose-dependent fashion. Treatment with 20 μM monacolin K achieved 57% inhibition ($p < 0.01$). To determine whether an increase in apoptosis was associated with the observed decrease in cell number after monacolin K treatment, the cells were stained with DAPI and analyzed by using a confocal microscope. As shown in Figure 1B, the nuclei of U937 cells exposed to monacolin K exhibited nuclear condensation and fragmented chromatin of typical apoptosis in a dose-dependent manner. Apoptosis was also detected by DNA fragmentation assay. DNA fragmentation was significantly increased after treatment with monacolin K in a dose-dependent manner (Figure 1C). Furthermore, the degree of apoptosis was quantified by analyzing the amount of sub-G1 DNA content in the U937 cells treated with monacolin K using an image cytometer. As shown in Figure 1D, in untreated control, the percentage of untreated control cells with fragmented DNA (sub-G1) was only 3%. Treatment with 20 μM monacolin K increased the percentage of cells with fragmented DNA (sub-G1) to 66%. Taken together, these findings indicated that exposure to monacolin K resulted in the inhibition of cell proliferation and a striking induction of apoptosis in U937 cells.

Monacolin K Down-regulated HMGCR Expression and Reduced Cholesterol Generation. To elucidate the effects of monacolin K on HMGCR production on the transcriptional level, cells were treated with various concentrations of monacolin K for 24 h. The cDNA was amplified by PCR with primers specific for HMGCR or GAPDH (as a control gene), and the results indicated that HMGCR mRNA expression was suppressed in the presence of monacolin K as shown in Figure 2A. The suppression of HMGCR mRNA expression correlated to Western blot analysis. Treatment of U937 cells with monacolin K

DOI: 10.1021/jf505275s
J. Agric. Food Chem. 2015, 63, 1186−1195

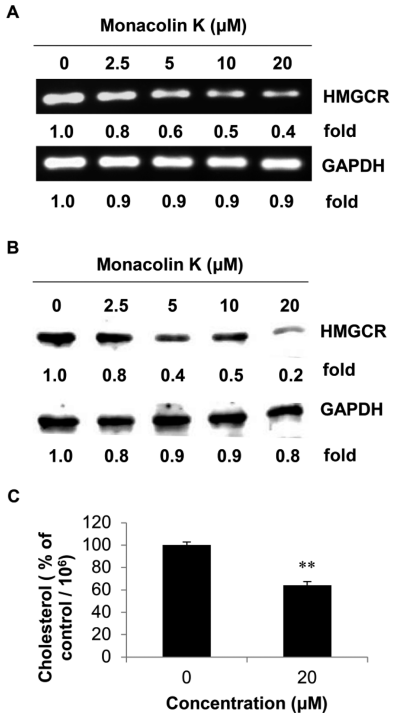

Figure 2. Monacolin K specifically suppresses HMGCR expression and cholesterol level in U937 cells. (A) Cells were incubated with various concentrations of monacolin K for 24 h, and HMGCR and GAPDH mRNA levels were analyzed by RT-PCR. (B) Immunoblots of whole cell lysates were probed with antibodies specific to HMGCR and actin. (C) U937 cells were treated with 20 μM monacolin K for 48 h, and the intracellular total cholesterol content was measured. All data represent means ± SD of triplicates (n = 3). In panel C, ** $p < 0.01$, compared with untreated cells (control groups).

inhibited HMGCR protein expression also in a dose-dependent manner (Figure 2B). After incubation with 20 μM monacolin K, we measured the intracellular total cholesterol content. As shown in Figure 2C, monacolin K showed significant inhibitory effect on cholesterol level at approximately 36% ($p < 0.01$), as compared with control cells.

Monacolin K Down-regulated GLO1 Expression and Increase MG Levels. To understand the critical roles of GLO1 in apoptosis, expression of GLO1 in U937 cells was monitored following treatment with monacolin K. U937 cells were treated with various concentrations of monacolin K for 48 h or 20 μM monacolin K for various times. The cDNA was amplified by PCR with primers specific for GLO1 or GAPDH (as a control gene). As shown in Figure 3A, monacolin K induced time- and dose-dependent down-regulation of GLO1 mRNA levels. Additionally, monacolin K administration resulted in a marked decrease in the GLO1 protein level as compared with control (Figure 3B). To investigate the effect of GLO1 expression blockage on MG level, U937 cells were treated with monacolin K at a concentration of 20 μM for 48 h. A significant increase in MG level was observed in comparison to levels produced by untreated cells (Figure 3C). Monacolin K caused an increase in MG accumulation by 2.7-fold as compared with that of control ($p < 0.05$).

Effects of Monacolin K on Ras Protein Expression and Downstream Signaling Pathways Regulation. Ras is considered a key protein for proliferative, survival, and oncogenic signals. We examined the regulatory effect of monacolin K on membrane protein Ras and its downstream signaling proteins, those being, Raf-1, Akt, and ERK. As shown in Figure 4A, after incubation with 20 μM monacolin K for 24 h, monacolin K significantly decreased the levels of H-Ras, K-Ras, N-Ras, and Raf-1 in cell membrane. In contrast, the H-Ras, K-Ras, N-Ras, and Raf-1 levels in cytosolic fraction were significantly higher in the monacolin K treatments. To assess whether monacolin K mediated and/or inhibited the phosphorylation of Akt and ERK, U937 cells were treated with various concentrations of monacolin K for 24 h. Figure 4B shows that monacolin K significantly inhibited the activation of Akt and ERK as shown by the decrease in the phosphorylation of Akt and ERK.

Monacolin K Abrogated NF-κB Signaling by Blocking the Nuclear Translocation of NF-κB (p65). To explore the underlying mechanism of NF-κB inactivation by monacolin K, we analyzed the protein expression of p65 by immunoblotting. As shown in Figure 5A, treatment of the U937 cells with 20 μM monacolin K for 24 h resulted in a significantly decreased level of p65 in the cell nucleus. In contrast, the p65 levels in cytosolic fraction were significantly increased. Confocal microscope analysis revealed that monacolin K inhibited p65 translocation from cytosol to nucleus (Figure 5B). Therefore, it was possible that the inhibitory effect of monacolin K on the NF-κB translocation was due to inactivation of Akt and ERK pathways, leading to a reduction in GLO1 expression.

Inhibitory Effects of Several Specific Inhibitors on Expression of Akt, ERK, and GLO1 and on Cell Viability in U937 Cells. Several specific inhibitors were used to assess whether a specific signaling pathway was involved in inhibition of monacolin K on GLO1 and other protein expressions. LY294002, U0126, and JSH-23 were used in the treatment of U937 cells. After treatment, cell extracts were prepared to determine the levels of GLO1. As shown in Figure 6A, three LY294002, U0126, and JSH-23 inhibitors could effectively suppress the GLO1 protein expressions. In addition, Figure 6B showed that Akt and ERK phosphorylation decreased after LY294002 and U0126 treatment for 24 h, and JSH-23 had little effect on the phosphorylation of Akt and ERK (Figure 6B). Next, we administered these inhibitors to U937 cells to determine whether suppression of the Ras/PI3K/Akt/NF-κB and Ras/Raf/ERK/NF-κB signaling pathways would inhibit cell viability. As shown in Figure 6C, these inhibitors had a strong inhibitory effect on U937 cell growth ($p < 0.01$). These results confirmed that the apoptotic effect of monacolin K followed the Ras/Akt/NF-κB/GLO-1 and Ras/Raf/ERK/NF-κB/GLO-1 signaling pathways.

Mevalonate Attenuated Monacolin K Induced Apoptosis and Protein Expression in U937 Cells. Accumulation of mevalonate, a precursor of cholesterol, has been reported to be associated with cell survival and proliferation of cancer cells. In the study, the treatment of mevalonate with monacolin K fully reversed its induced apoptosis in U937 cells as evidenced by DNA fragmentation and cell viability analysis ($p < 0.01$) (Figure 7A,B). Next, co-incubation of mevalonate with monacolin K for 24 h reversed monacolin K triggered loss of Akt and ERK phosphorylation (Figure 7C). We further investigated whether mevalonate blocked monacolin K suppresses GLO1 expression. After cells had been pre-incubated with mevalonate for 1 h and then treated with monacolin K for 48 h, as shown in Figure 7D,E, mevalonate prevented the decrease in GLO1 mRNA and protein by monacolin K. These results indicated that down-regulation of the mevalonate pathway is highly associated with monacolin K inhibition on GLO1 as well as the induction of apoptosis in U937 cells.

DOI: 10.1021/jf505275s
J. Agric. Food Chem. 2015, 63, 1186−1195

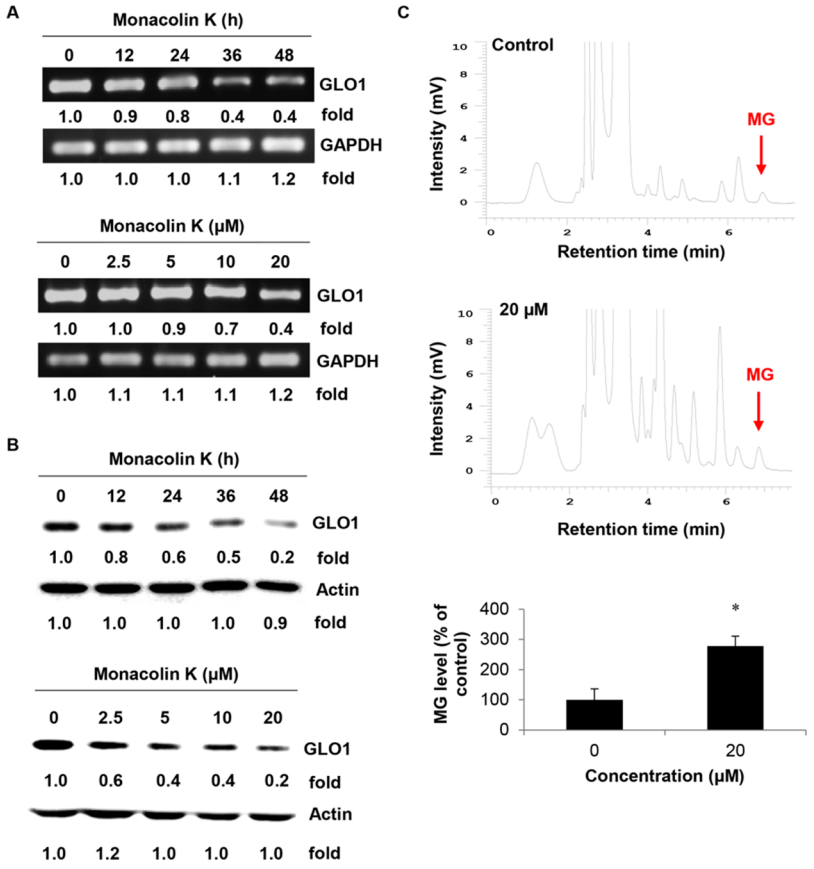

Figure 3. Down-regulation of GLO1 and increase MG levels by monacolin K in U937 cells. U937 cells were incubated with various concentrations of monacolin K for 48 h or with monacolin K (20 μM) for the indicated periods. (A) GLO1 and GAPDH mRNA levels were analyzed by RT-PCR. (B) Immunoblots of whole cell lysates were probed with antibodies specific to GLO1 and actin. (C) MG levels were estimated by HPLC as described under Materials and Methods. Monacolin K caused an increase in MG accumulation by 2.7-fold as compared with that of control (panel C). All data represent means ± SD of triplicates (n = 3). In panel C, ** $p < 0.05$, compared with untreated cells (control groups).

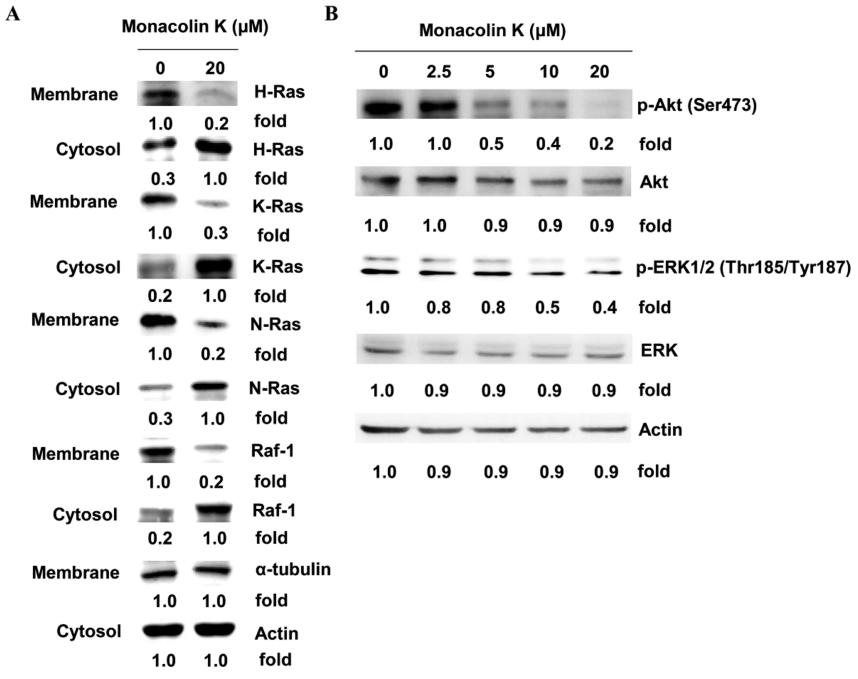

Figure 4. Down-regulation of Ras and its downstream signaling molecules by monacolin K in U937 cells. (A) After treatment with monacolin K for 24 h, membrane and cytosol proteins were extracted and used for immunoblotting of Ras (H, K, and N) and Raf-1. (B) Cells were lysed, and the total protein (30 mg) was submitted to SDS-PAGE and immunodetected with antiphospho- or anti-(ERK or Akt) antibodies. Tests were performed in triplicate and all experiments repeated three times (n = 3).

DOI: 10.1021/jf505275s
J. Agric. Food Chem. 2015, 63, 1186−1195

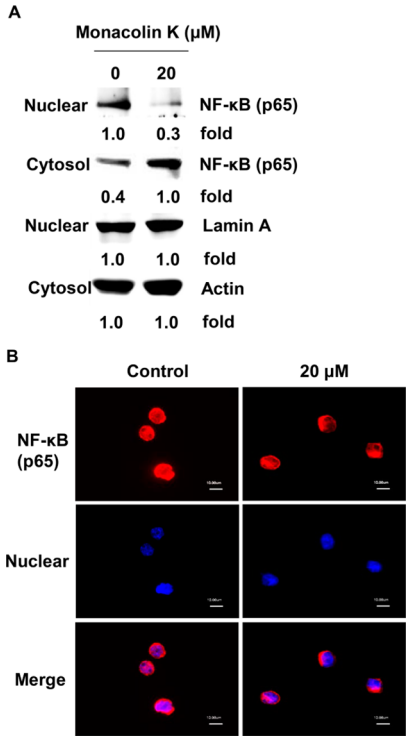

Figure 5. Monacolin K inhibits the translocation of NF-κB (p65) to the nucleus. (A) U937 cells were incubated for 24 h with indicated concentrations of monacolin K, and nuclear extracts were immunoblotted for p65 and the loading control lamin A. (B) After treatment for 24 h, cells were fixed, stained with p65 antibody and Alexa Fluor 594 goat anti-mouse (red), and counterstained with DAPI (blue). Tests were performed in triplicate and all experiments repeated three times (n = 3).

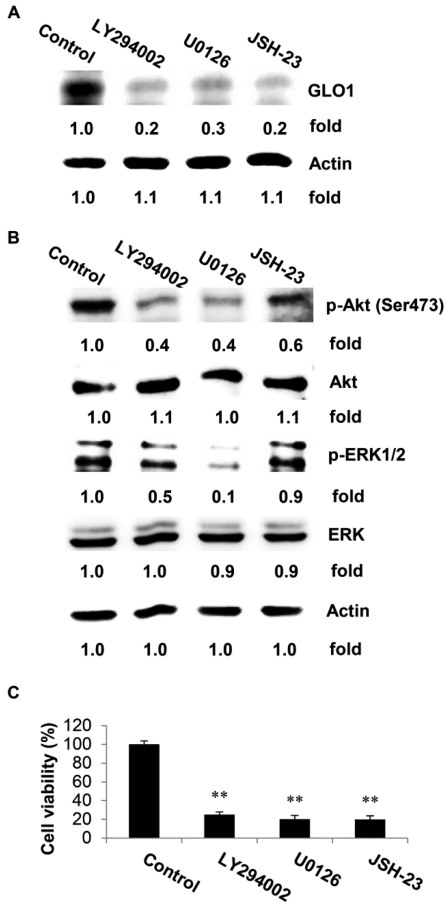

Figure 6. Down-regulation of Ras downstream signaling molecules and cell viability by various inhibitors in U937 cells. (A) U937 cells were treated with 20 μM of various inhibitors for 48 h. Total cell extracts were generated and immunoblotted with antibodies against GLO1. (B) U937 cells were treated with 20 μM of various inhibitors and incubated for 24 h; immunoblots of whole cell lysates were probed with antibodies specific to p-Akt and p-ERK. (C) The cell viabilities of U937 cells treated with 20 μM various inhibitors for 48 h were measured by MTT assay. All data represent means ± SD of triplicates (n = 3). In panel C, ** p < 0.01, compared with untreated cells (control groups).

DISCUSSION

The anticancer effect of monacolin K was demonstrated by its growth inhibitory activity on various cancer cell lines including human acute myeloid leukemia,[19] breast cancer,[20] and pancreatic cancer.[21] A structure−activity relationship analysis showed the alkyl functional group increased the lipophilicity of monacolin K, leading to a direct diffusion through the cell membrane, and affected cell proliferation, survival, and motility.[4] We hypothesize that monacolin K may induce apoptosis in U937 cells by inhibiting the mevalonate pathway and impairing Ras localization to the plasma membrane. It interrupted downstream Akt and ERK pathways, leading to the decreased HMGCR and GLO1 protein expressions.

Tumors, including leukemia, transformed from normal cells alter metabolism. Mutations of oncogenes and tumor-suppressor genes are believed to switch the glucose metabolism from oxidative phosphorylation to glycolysis in cancer cells.[22] Previous papers showed that cancer cells tend to use the glycolysis pathway to metabolize glucose due to lacking or mutated p53 gene.[23] Positron emission tomography (PET) data demonstrated that tumor cells accumulated extraordinary amounts of glucose. Elevated glucose metabolism is seen in activated lymphocytes in the draining lymph nodes of Moloney Murine Sarcoma and Leukemia Virus Complex-challenged mice using a ^{18}F-FDG probe.[24]

MG can be derived nonenzymatically from phosphorylated glycolytic intermediates dihydroxyacetone phosphate and glyceraldehyde-3-phosphate. MG causes DNA fragmentation at physiological concentrations in U937 cells[25] and HL-60 cell lines.[26] Recent studies have shown that MG specifically inhibits mitochondrial respiration in human leukemic leucocytes, leading to a tumoricidal effect.[27] We postulate that U937 cancer cell may use glycolysis to get the required energy and increase the GLO1 expression to eliminate excess MG for surviving and proliferation.

Detoxification of MG is mainly activated via the glyoxalase pathway present in the cytosol of all mammalian cells that use GSH as a cofactor.[28] The apoptotic effects of MG were found in high-glucose-treated VL-17A cells[29] and brain microvascular endothelial cells.[30] It has been shown that GLO1 expression was significantly up-regulated in prostate cancer LNCaP,[31] hepatocellular carcinoma,[32] and human gastric cancer,[33] when compared with adjacent nontumorous tissue. Recently, a novel mechanism of MG cytotoxicity in prostate cancer cells was proposed.[31] The silenced GLO1 in prostate LNCaP and PC3 cancer cells was found to be responsible for the accumulation of excess MG that led to the apoptosis via the cell survival NF-κB signaling pathway.

DOI: 10.1021/jf505275s
J. Agric. Food Chem. 2015, 63, 1186−1195

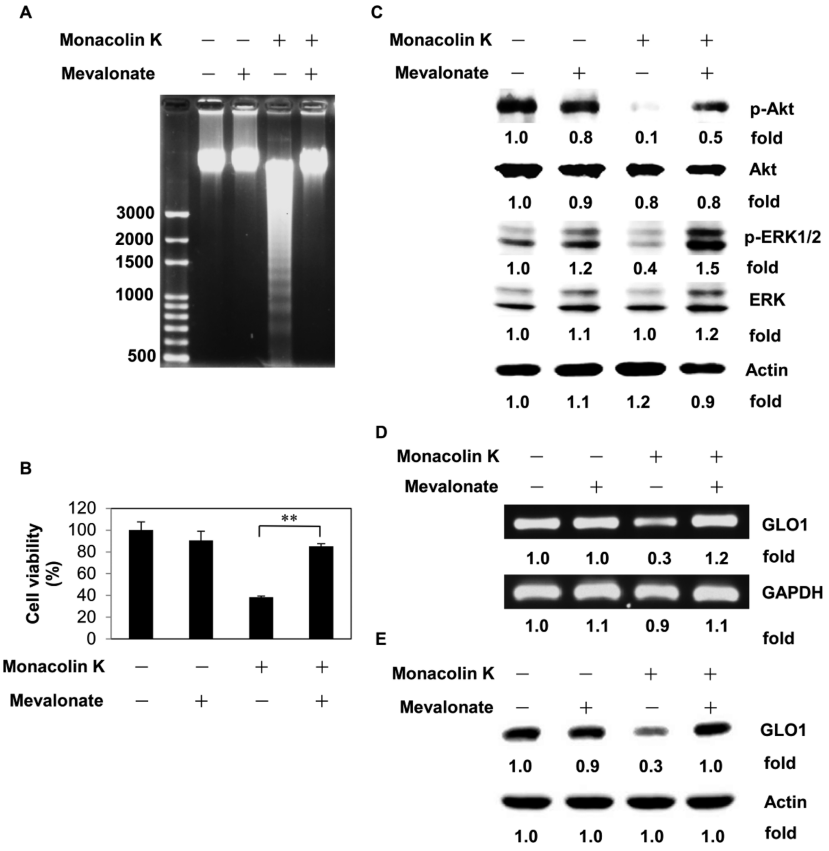

Figure 7. Recovery of monacolin K-induced apoptosis and suppression of Ras downstream signaling molecules in U937 cells by adding mevalonate. Cells were preincubated with 1 mM mevalonate for 1 h and then treated with 20 μM monacolin K for 48 h (A, B). (C) Cells were pretreated with 1 mM mevalonate for 1 h and then treated with 20 μM monacolin K for 24 h; immunoblots of whole cell lysates were probed with antibodies specific to antiphospho- or anti-(ERK or Akt). (D) GLO1 and GAPDH mRNA levels were analyzed by RT-PCR. (E) Immunoblots of whole cell lysates were probed with antibodies specific to GLO1 and actin. All data represent means ± SD of triplicates (n = 3). In panel C, ** $p < 0.01$, compared with untreated cells (control groups).

Ras has been reported to be frequently mutated in patients with AML. *Ras* gene mutation leads to the expression of activated Ras proteins and triggers constitutively overactive signaling inside the cell.[34] A previous study found N-Ras mutations (11%) and K-Ras mutations (5%) in AML patients.[35] Among the Ras isoforms, only H-Ras is palmitoylated and integrated into lipid rafts.[36] Activated Ras recruits Raf family proteins to the lipid raft and activates the subsequent ERK pathway. The constitutively activated Raf/MEK/ERK pathway has been characterized in both AML and acute lymphocytic leukemia (ALL).[37] Down-regulation of activated Raf proteins is closely related to cell cycle arrest in human promyelocytic leukemia and some hematopoietic cells. It is well established that the cross-talk between Ras/Raf/MEK/ERK and Ras/PI3K/PTEN/Akt pathways regulates cell growth and tumorigenesis in many leukemia samples.[38] Both pathways may trigger the phosphorylation of downstream targets and regulate cell survival and proliferation.

PI3K activity is another predominant growth factor activated pathway in varieties of human tumors including leukemia.[39] Accumulated evidence shows that PI3K is heavily involved in the malignant transformation of cells through the activation of the downstream Akt.[40] Blalock et al.[41] reported that MEK-mediated transformation of certain hematopoietic cells requires the activation of the PI3K pathway. Combined treatment with the Chk1 inhibitor 7-hydroxystaurosporine (UCN-01) and lovastatin was found to synergistically disrupt Ras prenylation and its translocation to membrane leading to the inhibition of the phosphorylation of both ERK 1/2 and Akt and enhanced apoptosis in U937 cells.[42] Using immunoprecipitation analysis, Chiu et al.[43] showed that Raf-1, Akt, and Ras can accumulate in the membrane to increase cell migration/invasion through PI3K/Akt and Raf-1/ERK activation. A redox modulated up-regulation of survival signaling, involving the ERK and PI3K/Akt phosphorylation pathways, has been reported in U937 cells.[44] Recent studies demonstrated that monacolin K can inhibit the Akt and ERK pathways leading to the decreased Bcl-2, whereas increased Bax expression in human colon carcinoma HCT-116 cell line.[45]

The expression and activity of the transcription factor NF-κB have been shown to be regulated by the Ras/PI3K/AKT and RAS/MAPK pathways.[46] The transcription factor NF-κB promotes cell proliferation and prevents apoptosis through its regulation of various gene products. Monacolin K and other natural statins were found to reduce NF-κB DNA-binding activity in tumor necrosis factor-α (TNF-α)-stimulated human myeloid leukemia KBM-5 cells.[47]

She et al.[48] reported that farnesyltransferase inhibitor manumycin A (manumycin) induced nitric oxide production and apoptosis in two myeloid leukemia cell lines (U937 and HL-60). Manumycin reduced the amount of functional Ras localized at the cytoplasmic membrane, thus blocking Raf-1 association with Ras. Manumycin inhibits the phosphorylation of both ERK1/2 and Akt and interferes with the association of PI3K and Ras in HepG2 cells.[49]

DOI: 10.1021/jf505275s
J. Agric. Food Chem. 2015, 63, 1186−1195

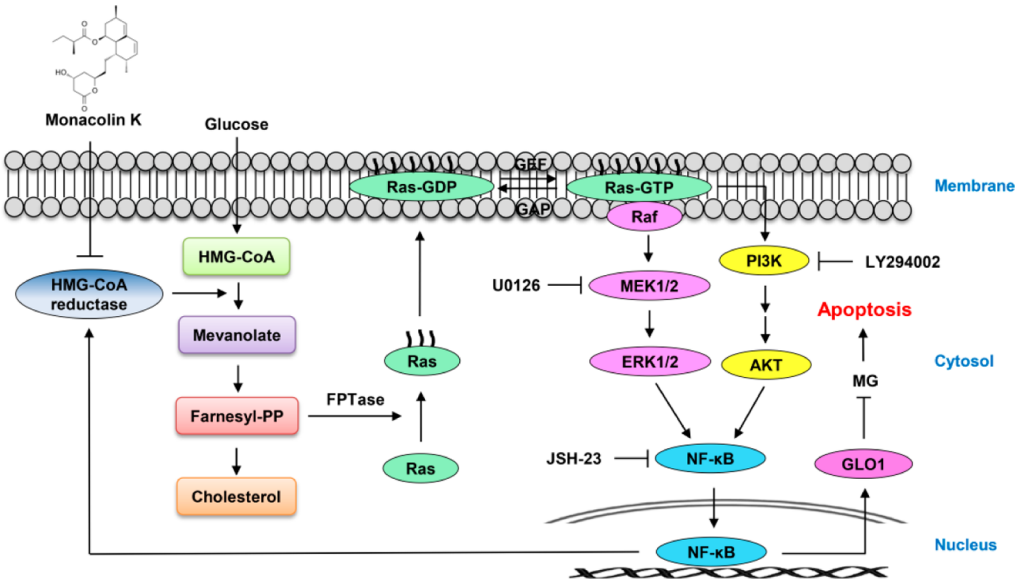

Figure 8. Diagram depicting the hypothesis of signaling regulation on GLO1 expression through both Ras/Raf/ERKNF-κB and Ras/PI3K/Akt/NF-κB pathways following monacolin K exposure in U937 cells. Farnesyl-PP, farnesyl pyrophosphate; FPTase, farnesyl prenyl transferase; GEF, guanine nucleotide exchange factor; GAP, GTPase-activating protein.

Monacolin K and other statins stimulate cell death, which was accompanied by the collapse of the mitochondrial membrane potential (MMP) in isolated Sprague–Dawley rat hepatocytes.[18] This observation indicates that cholesterol levels play a major role in the integrity of cell membranes, and the inactivation of HMGCR activity by monacolin K may be responsible for the apoptotic effect.

Our results reveal that the translocation of both Ras and Raf-1 to membrane and the levels of p-Akt in the PI3K/AKT/mTOR signaling pathway as well as p-ERK in the MAPK signal pathway were down-regulated by monacolin K in the U937 cell line. We postulate that monacolin K, a HMGCR inhibitor, blocks the biosynthesis of mevalonate and the subsequent farnesyl pyrophosphate through the inactivation of HMGCR. Lack of farnesyl pyrophosphate results in the inhibition of the isoprenylation of Ras protein and leads to the repression of accumulation of putative lipid raft-associated proteins. The subsequent phosphorylation of both Akt and ERK pathways will be thus abrogated. Overall, these results provided evidence of the specific molecular pathways by which monacolin K induces apoptosis: it decreases the activation of GLO1 and lowers cholesterol levels through the inhibition of Ras/Raf/ERK/NF-κB and Ras/Akt/NF-κB pathways (Figure 8). These findings provide evidence that it will be worthwhile to investigate the potential of monacolin K for the treatment of leukemia and potentially other types of human cancers.

AUTHOR INFORMATION

Corresponding Author

*(T.-C.H.) Mail: Department of Food Science, National Pingtung University of Science and Technology, 1 Shuehfu Road, Neipu, Pingtung 91201, Taiwan. E-mail: tchuang@mail.npust.edu.tw. Phone: +886-8-7703202, ext. 5196. Fax: +886-8-7740582.

Funding

This work was supported by the Ministry of Science and Technology (Taiwan) (NSC 103-2313-B-020-008-).

Notes

The authors declare no competing financial interest.

ABBREVIATIONS USED

GLO1, glyoxalase 1; HMGCR, HMG-CoA reductase; ERK, extracellular signal regulated kinases; Akt, protein kinase B; NF-κB, nuclear factor kappa-B; MG, methylglyoxal; RYR, red yeast rice

REFERENCES

(1) Ma, J.; Li, Y.; Ye, Q.; Li, J.; Hua, Y.; Ju, D.; Zhang, D.; Cooper, R.; Chang, M. Constituents of red yeast rice, a traditional Chinese food and medicine. *J. Agric. Food Chem.* **2000**, *48*, 5220–5225.

(2) Shamim, S.; Al Badarin, F. J.; DiNicolantonio, J. J.; Lavie, C. J.; O'Keefe, J. H. Red yeast rice for dysipidemia. *Mo. Med.* **2013**, *110*, 349–354.

(3) Hong, M. Y.; Seeram, N. P.; Zhang, Y.; Heber, D. Chinese red yeast rice versus lovastatin effects on prostate cancer cells with and without androgen receptor overexpression. *J. Med. Food* **2008**, *11*, 657–666.

(4) Zhu, L.; Yau, L. F.; Lu, J. G.; Zhu, G. Y.; Wang, J. R.; Han, Q. B.; Hsiao, W. L.; Jiang, Z. H. Cytotoxic dehydromonacolins from red yeast rice. *J. Agric. Food Chem.* **2012**, *60*, 934–939.

(5) Cheng-Qian, Y.; Xin-Jing, W.; Wei, X.; Zhuang-Lei, G.; Hong-Peng, Z.; Songde, X.; Pei-Lin, W. Lovastatin inhibited the growth of gastric cancer cells. *Hepatogastroenterology* **2014**, *61*, 1–4.

(6) van Besien, H.; Sassano, A.; Altman, J. K.; Platanias, L. C. Antileukemic properties of 3-hydroxy-3-methylglutaryl-coenzyme A reductase inhibitors. *Leuk. Lymphoma* **2013**, *54*, 2601–2605.

(7) Goldstein, J. L.; Brown, M. S. Regulation of the mevalonate pathway. *Nature* **1990**, *343*, 425–430.

(8) Swanson, K. M.; Hohl, R. J. Anti-cancer therapy: targeting the mevalonate pathway. *Curr. Cancer Drug Targets* **2006**, *6*, 15–37.

(9) Thornalley, P. J. Glutathione-dependent detoxification of α-oxoaldehydes by the glyoxalase system: involvement in disease mechanisms and antiproliferative activity of glyoxalase I inhibitors. *Chem.–Biol. Interact.* **1998**, *111–112*, 137–151.

(10) Kataoka, S.; Naito, M.; Tomida, A.; Tsuruo, T. Resistance to antitumor agent-induced apoptosis in a mutant of human myeloid leukemia U937 cells. *Exp. Cell Res.* **1994**, *215*, 199–205.

(11) Ranganathan, S.; Tew, K. D. Analysis of glyoxalase-I from normal and tumor tissue from human colon. *Biochim. Biophys. Acta* **1993**, *1182*, 311–316.

DOI: 10.1021/jf505275s
J. Agric. Food Chem. 2015, 63, 1186–1195

(12) Davidson, S. D.; Milanesa, D. M.; Mallouh, C.; Choudhury, M. S.; Tazaki, H.; Konno, S. A possible regulatory role of glyoxalase I in cell viability of human prostate cancer. *Urol. Res.* **2002**, *30*, 116−121.
(13) Hooper, N. I.; Tisdale, M. J.; Thornalley, P. J. Glyoxalase activity during differentiation of human leukaemia cells in vitro. *Leuk. Res.* **1987**, *11*, 1141−1148.
(14) Chaplen, F. W. Incidence and potential implications of the toxic metabolite methylglyoxal in cell culture: a review. *Cytotechnology* **1998**, *26*, 173−183.
(15) Bhattacharya, B. S.; Sweby, P. K.; Minihane, A. M.; Jackson, K. G.; Tindall, M. J. A mathematical model of the sterol regulatory element binding protein 2 cholesterol biosynthesis pathway. *J. Theor. Biol.* **2014**, *349*, 150−162.
(16) Vitols, S.; Norgren, S.; Juliusson, G.; Tatidis, L.; Luthman, H. Multilevel regulation of low-density lipoprotein receptor and 3-hydroxy-3-methylglutaryl coenzyme A reductase gene expression in normal and leukemic cells. *Blood* **1994**, *84*, 2689−2698.
(17) Mosmann, T. Rapid colorimetric assay for cellular growth and survival: application to proliferation and cytotoxicity assays. *J. Immunol. Methods* **1983**, *65*, 55−63.
(18) Wang, X.; Desai, K.; Clausen, J. T.; Wu, L. Increased methylglyoxal and advanced glycation end products in kidney from spontaneously hypertensive rats. *Kidney Int.* **2004**, *66*, 2315−2321.
(19) Park, W. H.; Lee, Y. Y.; Kim, E. S.; Seol, J. G.; Jung, C. W.; Lee, C. C.; Kim, B. K. Lovastatin-induced inhibition of HL-60 cell proliferation via cell cycle arrest and apoptosis. *Anticancer Res.* **1999**, *19*, 3133−3140.
(20) Klawitter, J.; Shokati, T.; Moll, V.; Christians, U.; Klawitter, J. Effects of lovastatin on breast cancer cells: a proteo-metabonomic study. *Breast Cancer Res.* **2010**, *12*, R16.
(21) Kusama, T.; Mukai, M.; Iwasaki, T.; Tatsuta, M.; Matsumoto, Y.; Akedo, H.; Inoue, M.; Nakamura, H. 3-Hydroxy-3-methylglutaryl-coenzyme a reductase inhibitors reduce human pancreatic cancer cell invasion and metastasis. *Gastroenterology* **2002**, *122*, 308−317.
(22) Koppenol, W. H.; Bounds, P. L.; Dang, C. V. Otto Warburg's contributions to current concepts of cancer metabolism. *Nat. Rev. Cancer* **2011**, *11*, 325−337.
(23) Cairns, R. A.; Harris, I. S.; Mak, T. W. Regulation of cancer cell metabolism. *Nat. Rev. Cancer* **2011**, *11*, 85−95.
(24) Shu, C. J.; Guo, S.; Kim, Y. J.; Shelly, S. M.; Nijagal, A.; Ray, P.; Gambhir, S. S.; Radu, C. G.; Witte, O. N. Visualization of a primary anti-tumor immune response by positron emission tomography. *Proc. Natl. Acad. Sci. U.S.A.* **2005**, *102*, 17412−17417.
(25) Okado, A.; Kawasaki, Y.; Hasuike, Y.; Takahashi, M.; Teshima, T.; Fujii, J.; Taniguchi, N. Induction of apoptotic cell death by methylglyoxal and 3-deoxyglucosone in macrophage-derived cell lines. *Biochem. Biophys. Res. Commun.* **1996**, *225*, 219−224.
(26) Kang, Y.; Edwards, L. G.; Thornalley, P. J. Effect of methylglyoxal on human leukaemia 60 cell growth: modification of DNA G1 growth arrest and induction of apoptosis. *Leuk. Res.* **1996**, *20*, 397−405.
(27) Biswas, S.; Ray, M.; Misra, S.; Dutta, D. P.; Ray, S. Selective inhibition of mitochondrial respiration and glycolysis in human leukaemic leucocytes by methylglyoxal. *Biochem. J.* **1997**, *323* (Part 2), 343−348.
(28) Abordo, E. A.; Minhas, H. S.; Thornalley, P. J. Accumulation of α-oxoaldehydes during oxidative stress: a role in cytotoxicity. *Biochem. Pharmacol.* **1999**, *58*, 641−648.
(29) Kumar, S. M.; Swaminathan, K.; Clemens, D. L.; Dey, A. GSH protects against oxidative stress and toxicity in VL-17A cells exposed to high glucose. *Eur. J. Nutr.* **2014**, DOI: 10.1007/s00394-014-0703-2.
(30) Li, W.; Maloney, R. E.; Circu, M. L.; Alexander, J. S.; Aw, T. Y. Acute carbonyl stress induces occludin glycation and brain microvascular endothelial barrier dysfunction: role for glutathione-dependent metabolism of methylglyoxal. *Free Radical Biol. Med.* **2013**, *54*, 51−61.
(31) Antognelli, C.; Mezzasoma, L.; Fettucciari, K.; Talesa, V. N. A novel mechanism of methylglyoxal cytotoxicity in prostate cancer cells. *Int. J. Biochem. Cell Biol.* **2013**, *45*, 836−844.
(32) Zhang, S.; Liang, X.; Zheng, X.; Huang, H.; Chen, X.; Wu, K.; Wang, B.; Ma, S. Glo1 genetic amplification as a potential therapeutic target in hepatocellular carcinoma. *Int. J. Clin. Exp. Pathol.* **2014**, *7*, 2079−2090.
(33) Hosoda, F.; Arai, Y.; Okada, N.; Shimizu, H.; Miyamoto, M.; Kitagawa, N.; Katai, H.; Taniguchi, H.; Yanagihara, K.; Imoto, I.; Inazawa, J.; Ohki, M.; Shibata, T. Integrated genomic and functional analyses reveal glyoxalase I as a novel metabolic oncogene in human gastric cancer. *Oncogene* **2014**, DOI: 10.1038/onc.2014.57.
(34) Beaupre, D. M.; Kurzrock, R. RAS and leukemia: from basic mechanisms to gene-directed therapy. *J. Clin. Oncol.* **1999**, *17*, 1071−1079.
(35) Bowen, D. T.; Frew, M. E.; Hills, R.; Gale, R. E.; Wheatley, K.; Groves, M. J.; Langabeer, S. E.; Kottaridis, P. D.; Moorman, A. V.; Burnett, A. K.; Linch, D. C. RAS mutation in acute myeloid leukemia is associated with distinct cytogenetic subgroups but does not influence outcome in patients younger than 60 years. *Blood* **2005**, *106*, 2113−2119.
(36) Hancock, J. F.; Paterson, H.; Marshall, C. J. A polybasic domain or palmitoylation is required in addition to the CAAX motif to localize p21ras to the plasma membrane. *Cell* **1990**, *63*, 133−139.
(37) Kornblau, S. M.; Womble, M.; Qiu, Y. H.; Jackson, C. E.; Chen, W.; Konopleva, M.; Estey, E. H.; Andreeff, M. Simultaneous activation of multiple signal transduction pathways confers poor prognosis in acute myelogenous leukemia. *Blood* **2006**, *108*, 2358−2365.
(38) McCubrey, J. A.; Steelman, L. S.; Abrams, S. L.; Bertrand, F. E.; Ludwig, D. E.; Basecke, J.; Libra, M.; Stivala, F.; Milella, M.; Tafuri, A.; Lunghi, P.; Bonati, A.; Martelli, A. M. Targeting survival cascades induced by activation of Ras/Raf/MEK/ERK, PI3K/PTEN/Akt/mTOR and Jak/STAT pathways for effective leukemia therapy. *Leukemia* **2008**, *22*, 708−722.
(39) Martinez-Lorenzo, M. J.; Anel, A.; Monleon, I.; Sierra, J. J.; Pineiro, A.; Naval, J.; Alava, M. A. Tyrosine phosphorylation of the p85 subunit of phosphatidylinositol 3-kinase correlates with high proliferation rates in sublines derived from the Jurkat leukemia. *Int. J. Biochem. Cell Biol.* **2000**, *32*, 435−445.
(40) Nicholson, K. M.; Anderson, N. G. The protein kinase B/Akt signalling pathway in human malignancy. *Cell. Signal.* **2002**, *14*, 381−395.
(41) Blalock, W. L.; Navolanic, P. M.; Steelman, L. S.; Shelton, J. G.; Moye, P. W.; Lee, J. T.; Franklin, R. A.; Mirza, A.; McMahon, M.; White, M. K.; McCubrey, J. A. Requirement for the PI3K/Akt pathway in MEK1-mediated growth and prevention of apoptosis: identification of an Achilles heel in leukemia. *Leukemia* **2003**, *17*, 1058−1067.
(42) Dai, Y.; Rahmani, M.; Pei, X. Y.; Khanna, P.; Han, S. I.; Mitchell, C.; Dent, P.; Grant, S. Farnesyltransferase inhibitors interact synergistically with the Chk1 inhibitor UCN-01 to induce apoptosis in human leukemia cells through interruption of both Akt and MEK/ERK pathways and activation of SEK1/JNK. *Blood* **2005**, *105*, 1706−1716.
(43) Chiu, C. F.; Ho, M. Y.; Peng, J. M.; Hung, S. W.; Lee, W. H.; Liang, C. M.; Liang, S. M. Raf activation by Ras and promotion of cellular metastasis require phosphorylation of prohibitin in the raft domain of the plasma membrane. *Oncogene* **2013**, *32*, 777−787.
(44) Vurusaner, B.; Gamba, P.; Testa, G.; Gargiulo, S.; Biasi, F.; Zerbinati, C.; Iuliano, L.; Leonarduzzi, G.; Basaga, H.; Poli, G. Survival signaling elicited by 27-hydroxycholesterol through the combined modulation of cellular redox state and ERK/Akt phosphorylation. *Free Radical Biol. Med.* **2014**, *77*, 376−385.
(45) Guruswamy, S.; Rao, C. V. Synergistic effects of lovastatin and celecoxib on caveolin-1 and its down-stream signaling molecules: implications for colon cancer prevention. *Int. J. Oncol.* **2009**, *35*, 1037−1043.
(46) Amiri, K. I.; Richmond, A. Role of nuclear factor-kappa B in melanoma. *Cancer Metastasis Rev.* **2005**, *24*, 301−313.
(47) Ahn, K. S.; Sethi, G.; Aggarwal, B. B. Reversal of chemoresistance and enhancement of apoptosis by statins through down-regulation of the NF-κB pathway. *Biochem. Pharmacol.* **2008**, *75*, 907−913.

DOI: 10.1021/jf505275s
J. Agric. Food Chem. 2015, 63, 1186−1195

(48) She, M. R.; Li, J. G.; Du, X.; Lin, W.; Niu, X. Q.; Guo, K. Y. [Involvement of mitochondria apoptotic pathway in the manumycin inducing apoptosis of U937 and HL-60]. *Zhonghua Xueyexue Zazhi* **2007**, *28*, 404−406.
(49) Zhou, J. M.; Zhu, X. F.; Pan, Q. C.; Liao, D. F.; Li, Z. M.; Liu, Z. C. Manumycin inhibits cell proliferation and the Ras signal transduction pathway in human hepatocellular carcinoma cells. *Int. J. Mol. Med.* **2003**, *11*, 767−771.

DOI: 10.1021/jf505275s
J. Agric. Food Chem. 2015, 63, 1186−1195